

Final Report
on ERA-Chemistry project NN117642 entitled
“Biomimetic synthesis of magnetic nanoparticles”

PI: Mihály Pósfai, University of Pannonia (Veszprém)

co-PI: Damien Faivre, Max Planck Institute for Colloids and Surfaces (Golm)

Table of contents:

Aims	2
Synergies between the Hungarian and German groups	2
Published and planned papers that resulted from this project	2
Results	3
(1) Synthesis of magnetic nanostructures on biological templates	3
<i>Concept</i>	3
<i>Creation of mutant filaments with functionalized sites on their surfaces</i>	4
<i>Attachment of magnetic nanoparticles to mutant filaments</i>	4
<i>Nucleation of magnetite on mutant filaments from iron-bearing solutions</i>	6
(1A) Broader implications of the particle nucleation and attachment experiments	7
(1B) Magnetic behavior of magnetite-covered filaments	8
(2) Magnetite mesocrystals and their chains produced by biomimetic synthesis	9
(2B) Magnetic properties of magnetite mesocrystals and magnetosome chains in bacteria, studied using electron holography	10
General comments	11
References cited	12

Aims

The primary aim of this collaborative project was to create one-dimensional magnetic nanostructures by **(1)** using biological filaments as templates for the attachment or growth of magnetic nanoparticles, and **(2)** to use biomimetic synthesis methods for the precipitation of magnetic particles that would self-assemble into linear structures. Secondary aims were **(A)** to obtain additional knowledge on the genetic control of biomineralization by magnetotactic bacteria, and **(B)** to characterize the magnetic properties of both natural and synthetic nanostructures.

Synergies between the Hungarian and German groups

While reaching aim (1) was the responsibility of the Hungarian side, aim (2) was mainly pursued by the German partner (at Max Planck Golm). To this date, we have published 4 papers in Q1 scientific journals (3 of them D1), one of which has both PIs as authors; nevertheless, the interaction of partners was highly beneficial in several other aspects beyond the issue of co-authorship. The German partner had experience in biomimetic synthesis that we partially lacked, while our expertise in transmission electron microscopy (TEM) was used by the partner. The exchange of know-how and materials, the organization of meetings where ideas could be shared and discussed, and joint involvement in new initiatives (such as a joint COST proposal, participation in an EU-Korea collaboration and initiating a new collaboration on magnetotactic bacteria) were all important for the success of the project. We also trained a PhD student from the German group in our lab to be able to perform electron tomography in a TEM. In addition, a third, associated partner (at the Ernst Ruska-Centre in Jülich) was also involved in the research, performing specialized TEM work towards secondary aim (B) above. Although this project formally terminated, the topic will be further pursued, and at least three more papers are expected to be submitted within a year, two of which will have joint authorship by the international partners. Below is a numbered list of published and planned papers, and the rest of this report is keyed both to the numbered aims above and to the specific papers.

Published and planned papers that resulted from this project

- #1. Bereczk-Tompa, É., Pósfai, M., Tóth, B., Vonderviszt, F. (2016) Magnetite-binding flagellar filaments displaying the MamI loop motif. **ChemBioChem**, 17, 2075-2082. DOI: 10.1002/cbic.201600377
- #2. Bereczk-Tompa, É., Vonderviszt, F., Horváth, B., Szalai, I., Pósfai, M. (2017) Biotemplated synthesis of magnetic filaments. **Nanoscale**, 9, 15062 – 15069. doi:10.1039/C7NR04842D.
- #3. Klein, Á., Kovács, M., Muskotál, A., Jankovics, H., Tóth, B., Pósfai, M., Vonderviszt, F. (2018) Nanobody-displaying flagellar nanotubes. **Scientific Reports**, 8:3584, doi:10.1038/s41598-018-22085-3.
- #4. Reichel, V., Kovács, A., Kumari, M., Bereczk-Tompa, É., Schneck, E., Diehle, P., Pósfai, M., Hirt, A.M., Duchamp, M., Dunin-Borkowski, R.E. and Faivre, D. (2017) Single crystalline superstructured stable single domain magnetite nanoparticles. **Scientific Reports**, 7, 45484, doi:10.1038/srep45484.
- *#5. Nagy, G., Papp, L., Pekker, P., Gomez Roca, A., Vonderviszt, F., Pósfai, M.: Effects of crystal morphology on the attachment of magnetite nanoparticles to protein filaments. To be submitted to Royal Society Interface.

*#6. Kovács, A., Pósfai, M., Li, Z-A., Caron, J., Prévèral, S., Lefèvre, C.T., Bazyliniski, D.A., Frankel, R.B., Dunin-Borkowski, R.E.: Influence of crystal shape and orientation on the magnetic microstructure of bullet-shaped magnetosomes synthesized by magnetotactic bacteria. To be submitted to Royal Society Interface.

*#7. Kuhrts, L., Macías-Sánchez, Prévost, S., Schneck, E., Pekker, P., Pósfai, M., Tarakina, N.V., Faivre, D.: Poly-L-arginine intervening in the crystallization pathway of magnetite. To be submitted.

*Planned papers have tentative titles and author lists. Additional studies may also result, but at this point these three papers are in a sufficiently advanced state to be cited here.

Results

(1) Synthesis of magnetic nanostructures on biological templates

Concept

In the original research plan we outlined a concept of creating filamentous biological templates for magnetic “coatings” by genetic engineering of the flagellin protein (Fig. 1). Tens of thousands of copies of the flagellin protein form the flagellum, the filamentous organelle of bacteria used for motion. A special feature of flagellin is that it self-assembles into filaments even *in vitro*. It was demonstrated previously that the D3 domain of flagellin can be replaced by suitably selected polypeptide sequences (Muskotál et al., 2010), without destroying the structure of the filament or the self-assembling ability of flagellin, thereby creating functionalized, periodically repeating sites on the surfaces of filaments. Our aim was to replace the D3 domain with fragments of proteins that were known or suspected to have magnetite- or iron-binding ability. Once these functionalized mutant filaments had been created, our plan was to use the filaments as templates for both the attachment of pre-made magnetite nanoparticles and for the heterogeneous nucleation and growth of magnetite from solution. The research was carried out entirely according to these plans.

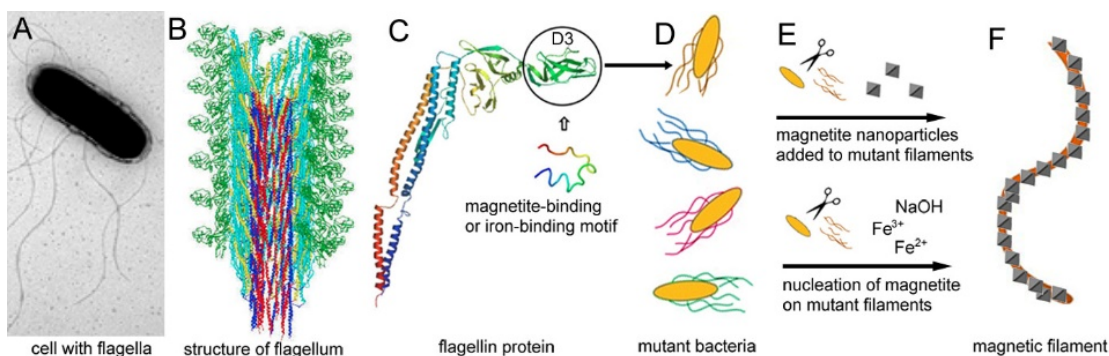


Fig. 1. Graphical illustration of the concept of our study. (A) Bacterial flagellar filaments are built of (B) thousands of flagellin subunits; (C) the D3 domain of flagellin can be replaced by specific binding motifs; (D) bacteria with mutant flagella are created, and (E) used in two different approaches (magnetite binding and magnetite nucleation) to produce (F) magnetic filaments.

Creation of mutant filaments with functionalized sites on their surfaces

The first step of the process shown in Fig. 1, the successful engineering of mutant bacterial flagella (Fig. 1D), i.e. that bacteria were able to grow the modified flagella, was demonstrated for four different protein fragments in paper #1 (two of which were specific to magnetotactic bacteria (MTB): the loop section of MamI and the C-terminal of Mms6) (Lohsse et al., 2014). The engineering of an additional two protein fragments and of two mutants with presumed neutral properties, to be used as controls, was described in paper #2 (Fig. 2). The lengths and thus the swimming abilities of mutant bacteria were highly variable (MamI_L produced short, straight flagellae, whereas IB2 had extremely long ones). In the last year of the project, we tested another three mutant variants, bringing the total number of engineered filaments to 11 (Table 1.)

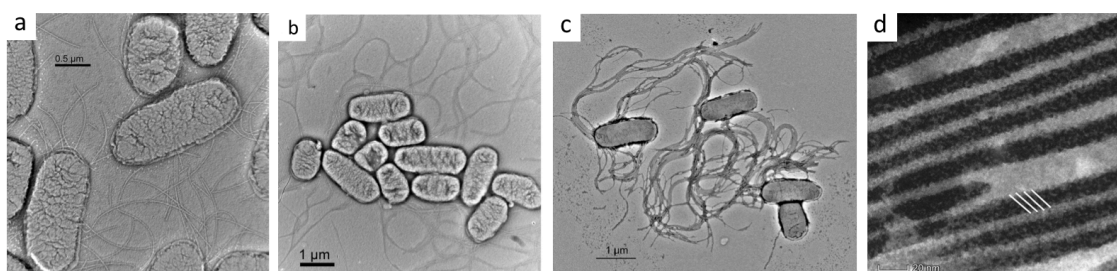


Fig. 2. Cells of *Salmonella* bacteria that possess genetically engineered, mutant flagella with inserted (a) MamI_L, (b) IB1 and (c) IB2 polypeptide sequences. (d) Dark-field scanning transmission electron microscopy (STEM) image of mutant filaments, showing periodic surface features about 5 nm apart, identified as the binding motifs.

peptide	ID	sequence	IP	expected result
MamI loop region	MamI_L	WWWSVTEFLRG	4.19	nucleation
Mms6 C-terminal region	Mms6_C	YAYMKSRDIESAQSDEE VELRDALA	6.00	nucleation
synth. magnetite-binding 1	SP1	SGVYKVAVDWQH	6.74	particle attachment
synth. magnetite-binding 2	SP2	TLNKPNRALHFN	11.00	particle attachment
synth. magnetite-binding 3	SP3	IPLPPSRPFFK	11.00	particle attachment
synth. magnetite-binding 4	SP4	QFSLPVAKLVNR	11.00	particle attachment
iron-binding 1	IB1	DLGEQYFKG	4.37	nucleation
iron-binding 2	IB2	HRDDDRHKDDKRKR	8.51	nucleation
iron-binding 3	IB3	HREERHKEEKR	8.60	nucleation
Δ D3_FliC_LETGPGEL	control1	LETGPGEL		no effect
Δ D3_FliC_GLNSA	control2	GLNSA		no effect
wild-type	control3			no effect

Table 1. Types, identification numbers, amino acid sequences, isoelectric points and expected functions of protein fragments that were used for preparing mutant bacterial filaments with either magnetite-binding (“particle attachment”) or iron-binding (“nucleation”) sites on their surfaces.

Attachment of magnetic nanoparticles to mutant filaments

The feasibility of route 1 to magnetic filaments (the upper cartoon in Fig. 1E), by the attachment of pre-made magnetite nanoparticles to the mutant filaments, was first demonstrated for MamI_L, SP1 and SP2. Contrary to expectation, Mms6_C did not

bind pre-made magnetite particles (paper #1). We performed a magnetic selection procedure to select the strongest binding variant, which turned out to be MamI_L. In addition, the attachment of magnetite particles to MamI_L filaments was qualitatively confirmed by using isothermal titration calorimetry. We produced magnetite-covered filaments both on flagella attached to cells and on flagellae that were mechanically removed from cells, and also on filaments that self-assembled *in vitro*. However, in all cases the filaments were not uniformly covered by the nanoparticles; fully covered and bare segments occurred, and to our surprise, the nanoparticles remained on the filaments in random crystallographic orientations instead of aligning themselves by the process typically termed “oriented attachment”.

In order to achieve a more uniform cover on the filaments, we experimented with various procedures of attaching the nanoparticles: microfluidic devices were used for ensuring a uniform flow of particles into the volume that contained the filaments, and magnetic fields were used for directing the movement of particles. However, these attempts did not significantly improve the magnetic coverage of filaments.

While in our first experiments (paper #1) we used magnetite nanoparticles produced by simple coprecipitation processes (and thus having mostly irregular shapes and sizes in the range between 10 and 20 nm), last year we experimented with particles having distinct, well-defined shapes and sizes (paper #5, in preparation). Our goal was to understand whether specific crystal faces such as the (111) (octahedron) and the (100) (cube) bind differently to the mutant filaments we created. The first step of this work was to produce magnetite particles with controlled shapes, which is most difficult in the case of cubes. We used organic reagents and solvents at high temperature to produce perfect octahedra; however, the experiments to produce cubes were only partly successful (in addition to cubes we also had octahedra in the samples). Therefore, we obtained magnetite nanocubes through our collaboration with our German partners, from a lab at U. Barcelona (Muro-Cruces et al., 2019).

The results of the experiments with cubes are surprising: not only did the magnetite nanocubes strongly attach to every type of mutant filament but also to the controls, including the wildtype. On the other hand, the octahedral nanoparticles attached only to certain mutants and showed no affinity towards the controls (Fig. 3). We interpret these observations as suggesting that the surface energies of specific crystal faces determine their affinity to bind to foreign surfaces: while the {111} octahedron is the equilibrium crystal form of magnetite, the {100} cube is a high-energy form, and therefore unstable and prone to bind to surfaces. These findings will be discussed in paper #5.

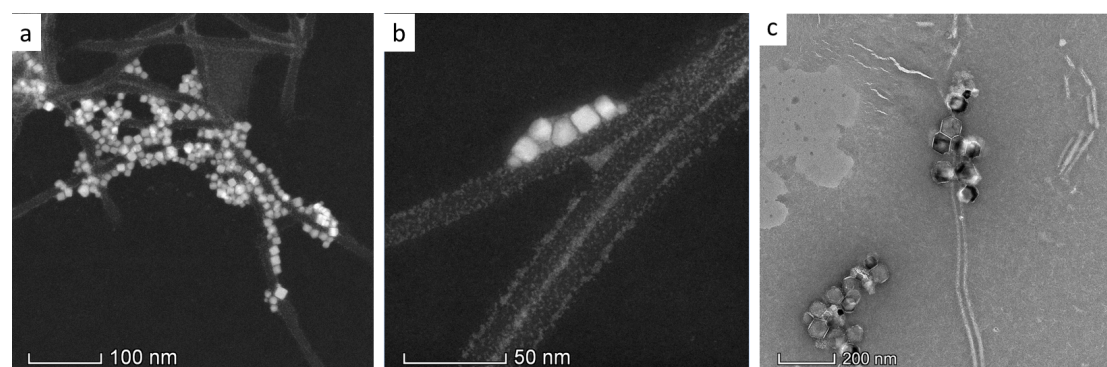


Fig. 3. (a) and (b) STEM dark-field images of magnetite nanocubes attached to the mutant filament IB2; (c) TEM bright-field image of magnetite octahedra, some of which are attached to a mutant filament, whereas a cluster of them (in the lower left) occurs separated from the filaments.

Nucleation of magnetite on mutant filaments from iron-bearing solutions

Following the route shown in the lower cartoon of Fig. 1E, we also performed nucleation experiments on mutant filaments. The solution contained both Fe(II) and Fe(III) ions, and by titrating a base to the solution, magnetite precipitated. Again, we expected heterogeneous nucleation of magnetite on the filaments to produce uniform cover, resulting in magnetic nanotubes. Instead, the filaments were again partially covered, and the magnetite particles had random orientations. Compared to the particle attachment experiments, the nucleation experiments produced a broader size distribution, and very small (<5 nm) particles also occurred (Fig. 4). The results of these experiments were presented and discussed in paper #2.

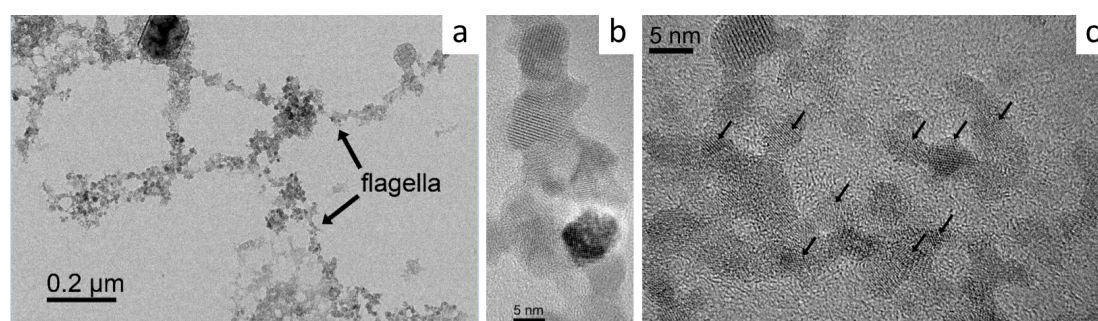


Fig. 4. Results of nucleation experiments on Mms6_C mutant filaments; (a) filaments covered by magnetite nanoparticles, (b) random crystallographic orientations of >5 nm particles on a filament; (c) 1 to 5-nm large magnetite particles on the filament template.

Filament sample	Expected result	Magnetite nucleation	Magnetite binding	
			octahedra	cubes
Maml_loop	nucleation	yes	yes	yes
Mms6_Cterm	nucleation	yes	no	
SP1	binding	yes	yes	
SP2	binding		yes	
SP3	binding		yes	yes
SP4	binding	yes	yes	yes
IB1	nucleation	yes	no	
IB2	nucleation		no	yes
IB3	nucleation	yes	no	
Δ D3_FliC_LETGPGE (control)	no effect	yes	no	yes
Δ D3_FliC_GLNSA (control)	no effect	no	no	
wild-type (control)	no effect	no	no	yes

Table 2. Expected and observed results of magnetite nucleation and attachment experiments, the latter performed with both octahedral and cube-shaped particles. The red font indicates results that were unexpected.

A summary of the results of particle attachment and nucleation experiments reveals that nucleation is less specific than the binding of octahedral magnetite particles (Table 2). Except for the wildtype and another control filament, magnetite nucleated on all filaments, even on the ones that were designed to function as surfaces for particle attachment (marked in red in Table 2). However, the attachment of cube-shaped magnetite particles is the least specific process, since the nanocubes attach to everything.

(1A) Broader implications of the particle nucleation and attachment experiments

Although nucleation from solution and attachment of nanoparticles to a pre-existing surface are typically considered two different processes, non-classical crystal nucleation pathways have been increasingly recognized in various systems (Gebauer and Cölfen, 2011), and in many cases nucleation and particle attachment cannot be clearly distinguished. We believe this is the case in the above experiments as well: in the nucleation experiments “prenucleation clusters” probably formed in the solution and then attached to the filaments – such clusters could have resulted in the 2–5 nm large, randomly oriented particles that we observed. Simple coulombic interactions between the protein and iron ions in solution cannot explain the observations (see the cases marked in red in Table 1). An alternative interpretation is offered if clusters instead of ions are attracted to the filaments from solution. Since ionic clusters can have either positive or negative charges, they will be attached to any charged amino acid on the filament surface, making “nucleation” rather non-specific.

Mms6 from magnetotactic bacteria (MTB) has been the most widely used magnetite-nucleating protein in experiments that aimed at producing magnetite nanoparticles with controlled properties or in pre-designed patterns (Prozorov et al., 2013). The magnetite-nucleating ability of Mms6 is usually attributed to its Asp(D) and Glu(E) amino acids attracting iron cations from solution. In the case of Mms6, our experiments confirmed its nucleating ability but no affinity to anchor octahedral magnetite nanoparticles. The loop section of MamI, however, turned out to be efficient in both nucleation and particle attachment experiments. We assume the strong binding of MamI to magnetite (as shown by ITC) might have a role in localizing the growing magnetite nanocrystal to the membrane of the magnetosome vesicle.

In general, the prevailing view of biomineralization in MTB is that each specific magnetosome membrane protein has a specific function, such as Mms6 is responsible for magnetite nucleation, other proteins for crystal shape control, etc. Based on our results, the question arises whether the roles of magnetosome proteins in MTB should be viewed from a reverse angle: the challenge for the bacterium is not the nucleation of magnetite (since it nucleates on almost anything) but controlling the nucleation of *only one* crystal in each magnetosome vesicle. Perhaps the role of some of the membrane proteins is actually the inhibition of the attachment of ionic clusters. At this point, our reasoning is only speculation, but in the future we plan to devise experiments for studying the distinct stages of biomineralization.

Input from this project was also used in efforts to improve the design of flagellin constructs. The applicability of a procedure to obtain filaments with molecular recognition capability was demonstrated by inserting single-domain antibodies in place of the D3 domain of flagellin. The results were published in paper #3.

(1B) Magnetic behavior of magnetite-covered filaments

The magnetic nanofilaments that were produced in the first process (by nanoparticle attachment) were subjected to bulk magnetic measurements. When an external magnetic field is applied, the filaments form large bundles, aligned parallel to the field direction (Fig. 5A). In order to test the magnetic consequences of the special property of these structures (their elongated, filamentous nature), we tested changes in the viscosity of their suspension in magnetic fields. By applying a strong magnetic field perpendicular to the flow, the viscosity of the filament-bearing solution increased twofold, whereas those of the controls (suspension of wild-type filaments and magnetic nanoparticles without filaments) remained unchanged (Fig. 5B).

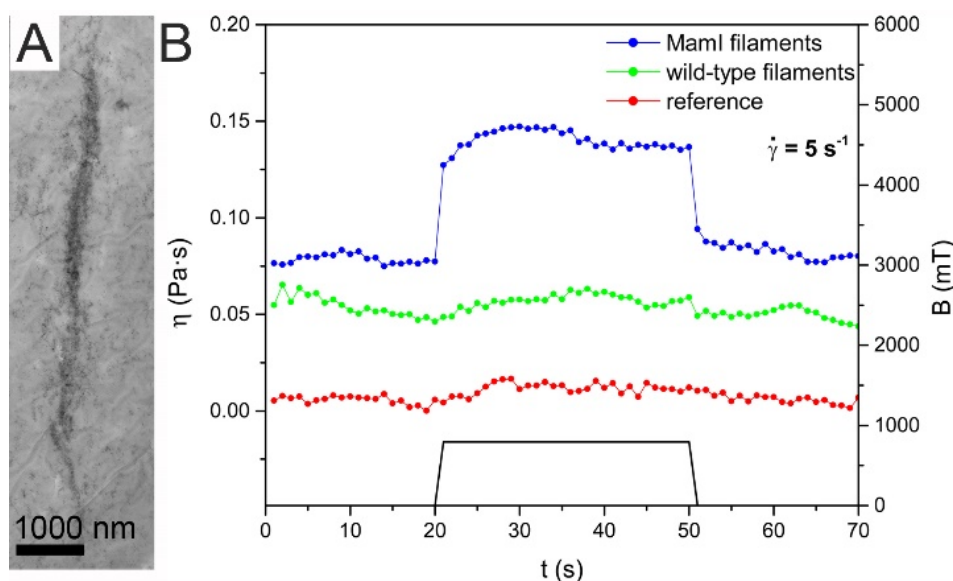


Fig. 5. A) Bright-field TEM image of magnetite-covered FliC-MamI_L filaments that were subjected to a static magnetic field of 800 mT when deposited onto the sample substrate. The magnetic filaments aligned in “ropes” (seen as a dark band in the image), composed of bundles of smaller chains of magnetite-covered filaments. (B) Viscosity of a solution containing magnetic nanofibers (blue), compared to the viscosities of two reference solutions, one of which contained the same amount of magnetite but no filaments (red), and another that contained magnetite nanoparticles and wild-type (unmodified) filaments (green). The samples were exposed to an external magnetic field of 800 mT for 30 s (as shown by the black line). The viscosity of the solution containing magnetic nanofibers increased when the magnetic field was turned on, whereas the viscosities of the two reference solutions remained constant.

Currently, we have no clear agenda for a technological or medical use of the magnetic filaments. Elongated magnetic particles might be useful for magnetic particle imaging in MRI, and webs of fibers loaded with magnetic nanoparticles have been suggested as excellent materials for cancer therapy through hyperthermia (Huang et al., 2012). The alignment of magnetic fibers by an external field might be used for creating a fluid with a magnetically controllable viscosity; however, for any of these applications, a more uniform coverage of filaments by nanoparticles would be needed. A novel idea is to use magnetosome chains for building spin wave logic circuits, thereby achieving nanoscale magnonic devices instead of currently available micrometer-scale patterns (Zingsem et al., 2019); with a better control of size and coverage, our magnetic filaments might be also suitable for such applications.

(2) Magnetite mesocrystals and their chains produced by biomimetic synthesis

The German partner synthesized monodisperse (about 40 nm diameter) magnetite mesocrystals in the presence of an organic additive (polyarginine). The term “mesocrystal” refers to particles that are composed of crystalline subunits that became aggregated by sharing a common crystallographic orientation. The formation of mesocrystals was found to take place in a three-stage process: (1) 2-nm primary particles form from solution, then (2) aggregate to form 10-nm single crystals of magnetite, which (3) form 40-nm particles by oriented attachment. These particles do not continue to grow; instead, new particles nucleate. The produced mesocrystals provide us with a unique opportunity to study some fundamental problems of nanoparticle magnetism, e.g., whether the magnetic properties of the 40-nm particles reflect the sizes of the mesocrystals (which are within the stable single domain size range) or those of their 10-nm subunits (which are within the superparamagnetic size range). In addition, the 40-nm mesocrystal particles tend to self-assemble into linear chains in fluids and on a surface, thereby providing an opportunity to study the magnetism of chains of mesocrystals. We were involved in the TEM characterization of the structures of the products, and through our Jülich collaboration, in the analysis of magnetic properties. These results were published in paper #4.

In order to better understand the effect of the organic additive on magnetite mesocrystal formation, the reaction was further studied last year, under systematically varied synthesis conditions, and by analyzing the structures of the particles *in situ*, using small-angle X-ray scattering in a synchrotron beamline. By changing the pH the sizes of particles could be tuned, and thereby the magnetic properties could be changed (from superparamagnetic to stable single domain state). An important aspect of this work is the proper characterization of mesocrystal morphology and structure, which was done in our new Nanolab, using electron tomography (Fig. 6). A first draft of the paper with the above results has been prepared and will be submitted this year (paper #7).

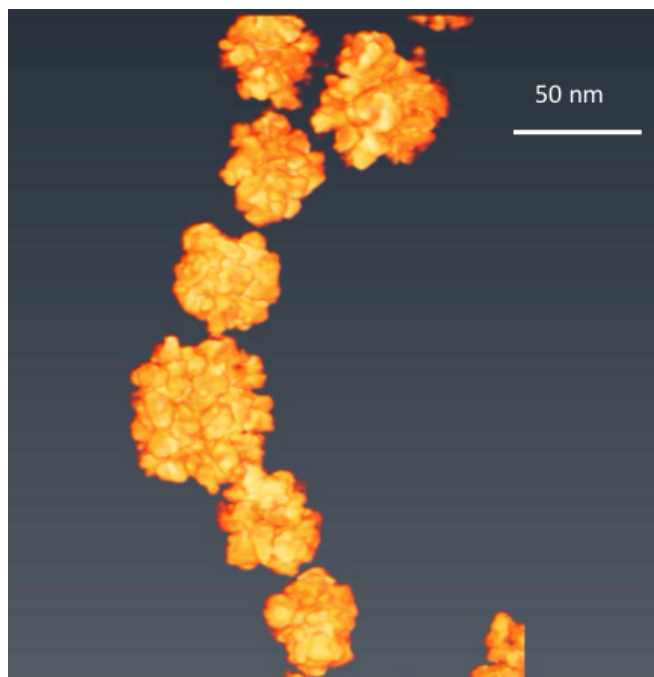


Fig. 6. 3D morphologies of magnetite mesocrystals, self-arranged in a chain, reconstructed from an electron tomography experiment (from a tilt-series of dark-field STEM images).

(2B) Magnetic properties of magnetite mesocrystals and magnetosome chains in bacteria, studied using electron holography

In collaboration with the Jülich Research Center we used electron holography (EH) to study the magnetic induction of the mesocrystals described above. Most particles contain a single magnetic domain, suggesting that the magnetic properties of the mesocrystals reflect those of the entire entity instead of those of the smaller subunits (which would be superparamagnetic if they were isolated). In other words, even though each 40-nm particle is composed of distinct subunits, the entire particle can be regarded as a single crystal both structurally and magnetically (Fig. 7; paper #4).

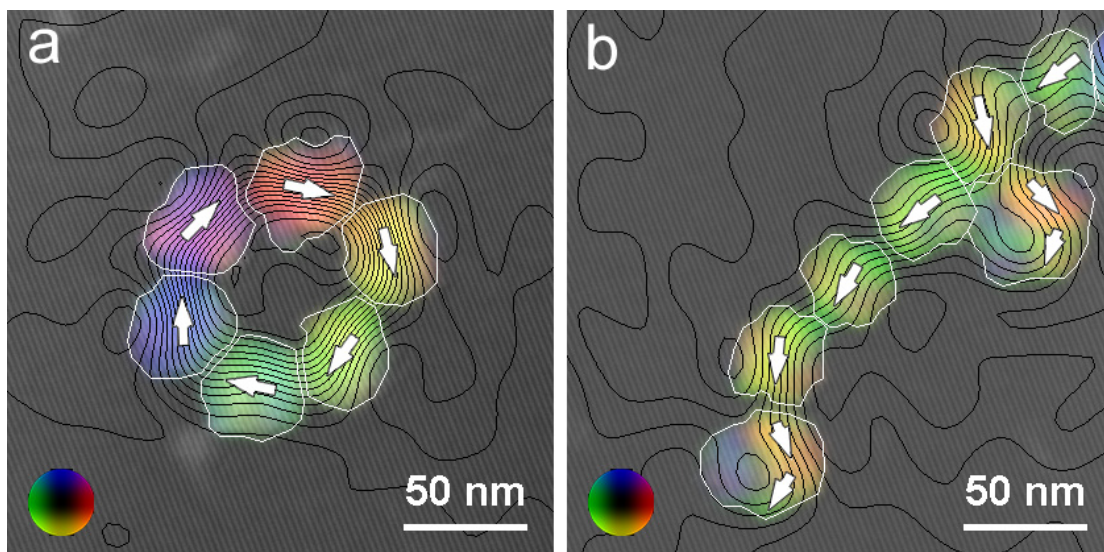


Fig. 7. Magnetic induction maps recorded using off-axis electron holography from (a) a ring and (b) a chain of magnetite particles. The colours and contours show the direction and strength of the projected in-plane magnetic flux density, respectively. A colour wheel is shown as an inset at the lower left corner of each image. The white arrows indicate the direction of the magnetic induction in each particle. A thin white line marks the outer edge of each particle.

Another, related line of research is also pursued with the Jülich partner: the magnetic properties of natural, elongated magnetite particles and their chains (from magnetotactic bacteria) are studied. Cells of magnetotactic bacteria are used as model systems for studying the magnetic properties of ferrimagnetic nanocrystals. Each bacterial strain produces magnetosomes (membrane-bound magnetic nanocrystals) that have distinct sizes, shapes, crystallographic orientations and spatial arrangements, thereby providing nanoparticle systems whose distinct magnetic properties are unmatched by synthetic samples. We used EH in the TEM to study the magnetic properties of both isolated and closely-spaced *bullet-shaped* magnetite magnetosomes. We studied bacterial strains RS-1, LO-1 and HSMV-1, which produce magnetite magnetosomes whose crystallographic axes of elongation are parallel to one (or any) of the $\langle 100 \rangle$ (RS-1 and LO-1) or $\langle 110 \rangle$ (HSMV-1) directions. We showed that the particles each contain a single magnetic domain and measured the projected in-plane magnetization distributions and magnetic moments of individual particles.

In an isolated particle, the magnetic induction is strictly confined to be parallel to its elongation axis, irrespective of the crystallographic direction that is parallel to the

direction of elongation. Since $\langle 111 \rangle$ is the magnetic easy axis in magnetite at room temperature, the shape anisotropy of the particle overrides the effect of crystal-structure-related anisotropy. In some disordered chains, bullet-shaped crystals occur side by side, with their long axes either parallel or perpendicular to each other. In such cases, magnetostatic interactions between the particles can result in some of the bullet-shaped magnetosomes being magnetized perpendicular to their direction of elongation. Thus, our work established the hierarchy of competing magnetic effects – shape and magnetocrystalline anisotropy and magnetostatic interactions – that determine the magnetization of both single nanoparticles and their chains.

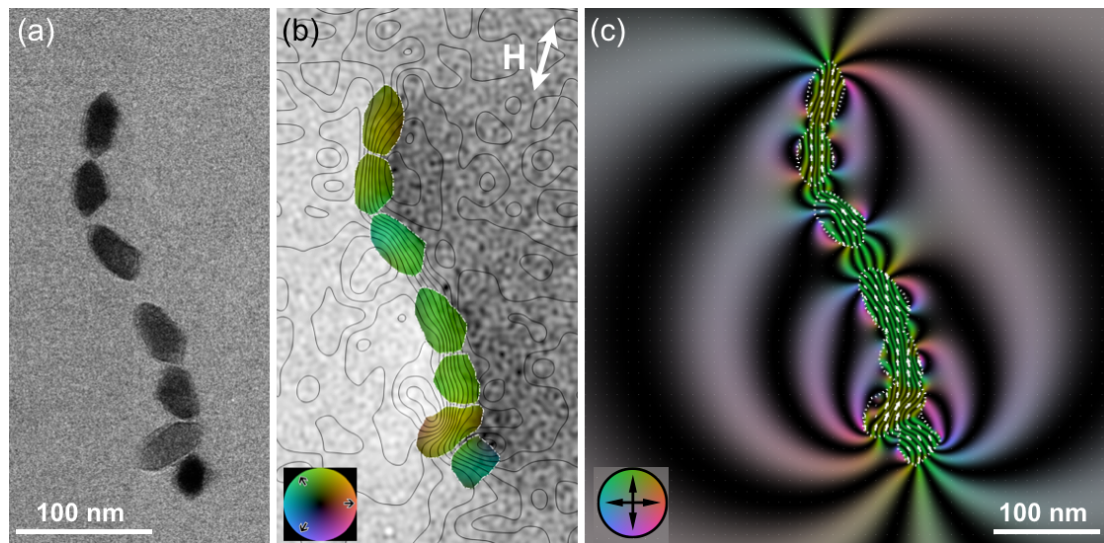


Fig. 8. Analysis of magnetic properties of magnetosomes of strain RS-1. (a) BF TEM image of a chain of magnetosomes and (b) a corresponding magnetic induction (\mathbf{B}) map recorded using off-axis EH after saturating the sample magnetically in the direction of the double-headed arrow marked H . Magnetic phase contours of spacing 0.0375 radians and the outlines of the positions of the magnetosomes are marked. Colors indicate the direction of the magnetic induction, according to the color wheel (lower left). (c) Calculated projected magnetization (\mathbf{m}) map of the magnetosomes and stray field.

Based on the above results, a complete manuscript was produced already three years ago, intended for Royal Society Interface (paper #6); however, the PI of the Jülich group wishes to add micromagnetic modeling (to be used for a comparison with experimental data), but to this date, he has not been able to find the time needed to complete the project. Nevertheless, we hope the work can be submitted by the end of this year.

General comments

In this project we produced new scientific results along the following lines:

- genetically engineered mutant bacterial filaments with specifically designed functional sites on their surfaces;
- used these filaments as templates for the attachment and nucleation of magnetic nanoparticles;
- by doing this we produced magnetic nanofibers, and
- gained new knowledge both on the functions of the Mms6 and MamI proteins in magnetotactic bacteria and on the nucleation of crystalline nanoparticles

- from solutions in general;
- participated in research that produced magnetic mesocrystals and their chains, and
- we characterized the structural, chemical and magnetic properties of these mesocrystals;
- studied and characterized the magnetic properties of elongated, bullet-shaped magnetosomes from magnetotactic bacteria.

In addition to the above results the project was highly useful for providing science projects for students. Éva Bereczk-Tompa completed her PhD (her thesis and pre-defence were judged as excellent by two external reviewers; sadly, for health issues she decided to withdraw from pursuing the title). Two other PhD students have been involved in the research (Zsófia Békéssy and Zsombor Molnár). Two BSc student theses (by Anett Lázár and Lejla Papp) also resulted from this project. We trained two international PhD students: Lenka Fialova spent 6 months at the University of Pannonia studying genetic engineering techniques, and Lucas Kuhrts spent some weeks at UP for studying electron tomography.

The project also helped us recruit two scientists who arrived to Veszprém from Debrecen and Miskolc (Dr. Georgina Nagy and Péter Pekker, respectively), and were temporarily funded by the project. Dr. Georgina Nagy is a biologist who was hired to replace Éva Tompa to perform the genetic engineering work within this project, and Péter Pekker is an electron microscope specialist whose expertise benefited the project greatly.

During the course of the project a brand new electron microscopy laboratory was established at UP (the “Nanolab”) under the leadership of the PI. This is a major progress in research infrastructure, and the ERA project was useful for providing immediate science problems for the new lab and, on the other hand, benefited greatly from the new facilities. The new Nanolab guarantees that international science cooperation between our group and the partners in this project will continue in the future, and collaboration will be extended to a range of related science problems and potentially to other foreign research groups.

In all, the project helped us greatly in the last four years to perform international-level research, and we are grateful to the reviewers and the panels of NKFIH for supporting our original proposal, and the administrative personnel of NKFIH for their prompt and flexible handling of issues that arose during the course of research.

References cited

- Gebauer, D. and Cölfen, H.: Prenucleation clusters and non-classical nucleation. *Nano Today*, 6, 564-584, 2011.
- Huang, C., Soenen, S. J., Rejman, J., Trekker, J., Chengxun, L., Lagae, L., Ceelen, W., Wilhelm, C., Demeester, J., De Smedt, S. C.: Magnetic electrospun fibers for cancer therapy. *Adv. Funct. Mater.*, 22, 2479–2486, 2012.
- Lohsse, A., Borg, S., Raschdorf, O., Kolinko, I., Tompa, É., Pósfai, M., Faivre, D., Baumgartner, J., and Schüller, D.: Genetic dissection of the mamAB and mms6 operons reveals a gene set essential for magnetosome biogenesis in *Magnetospirillum gryphiswaldense*, *J. Bacteriol.*, JB. 01716-01714, 2014.

- Muro-Cruces, J., Roca, A.G., López-Ortega, A., Fantechi, E., del-Pozo-Bueno, D., Estradé, S., Peiró, F., Sepúlveda, B., Pineider, F., Sangregorio, C. and Nogues, J.: Precise size control of the growth of Fe₃O₄ nanocubes over a wide size range using a rationally designed one-pot synthesis. *ACS Nano*, 13, 7716-7728, 2019.
- Muskotál, A., Seregélyes, C., Sebestyén, A., and Vonderviszt, F.: Structural basis for stabilization of the hypervariable D3 domain of *Salmonella* flagellin upon filament formation, *J. Mol. Biol.*, 403, 607-615, 2010.
- Prozorov, T., Bazylinski, D.A., Mallapragada, S.K. and Prozorov, R.: Novel magnetic nanomaterials inspired by magnetotactic bacteria: Topical review. *Materials Science and Engineering: R: Reports*, 74, 133-172, 2013.
- Zingsem, B.W., Feggeler, T., Terwey, A., Ghaisari, S., Spoddig, D., Faivre, D., Meckenstock, R., Farle, M. and Winklhofer, M.: Biologically encoded magnetics. *Nature Communications*, 10, 1-8, 2019.